# Grasp Planning based on Dynamics Shaping

Tasuku Yamawaki and Masahito Yashima

*Abstract*— **The present paper proposes a novel grasp planning for a robotic hand to achieve a manipulation task with high accuracy against unknown disturbances. In precision tasks such as a peg-in-hole insertion or a manipulation with a tool, the manipulation accuracy of the task frame on the grasped target is important. We verify that the manipulation task accuracy for the robot hand system against unknown disturbances is determined by the direction of the singular vector and condition number of the output controllability matrix for the manipulation system. The grasp planning based on dynamics shaping is proposed, which finds a grasp configuration so that the error of the task coordinate position toward the direction which requires the high positional precision can be suppressed. The validity of the grasp planning is shown by several simulations concerning a peg-in-hole insertion task.**

## I. Introduction

The practical robot task such as an assembly task is operated by the collaboration between a robot arm and a robot hand. The robot arm performs a global motion to move the robot hand along the desired path. In contrast, the robot hand as shown in Fig. 1 performs a local motion such as manipulating precisely the grasped object or tool toward the specific direction. In general, a robot system shares its manipulation task between the robot arm and the robot hand as described above.

In a model based control for manipulation task, uncertainties of the manipulation system often deteriorate the manipulation task accuracy. For example, unpredictable friction of joints, mechanical backlash, etc., which cannot be modeled, are applied to robot systems as unknown disturbances and affect seriously its manipulation task accuracy. To enable a precise manipulation, it is desired to plan the motion and grasp which can ensure high task accuracy against the unknown disturbances. However, to our knowledge, there has been few study on such planning.

We have proposed the novel motion planning based on "dynamics shaping", the concept of which is to shape the robot dynamics appropriately by changing its configuration in order to achieve the robust motion against the unknown disturbances. The dynamics shaping has been applied to plan the robot arm's global motion such as the hitting motion [12] and the tracking motion [13].

In this paper, we deal with the local and precise motion performed by a robot hand. The robot hand is also required to grasp the object or tool so that the task coordinate specified on the object (Fig. 1) can be robust against the unknown disturbances along the direction where the manipulation task accuracy is required. To obtain such a grasp configuration, this paper proposes the grasp planning based on "dynamics shaping".

The authors are with Dept. of Mechanical Systems Engineering, National Defense Academy of Japan, 1-10-20, Hashirimizu, Yokosuka, JAPAN {yamawaki, yashima}@nda.ac.jp

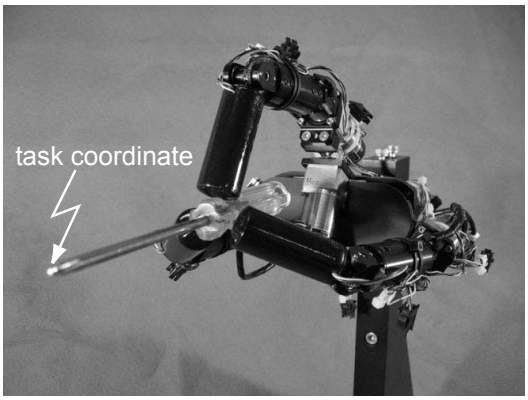


Fig. 1. The NDA Hand executing a precise manipulation task

To optimize grasp configuration, various evaluation criteria have been introduced for manipulation tasks by the robot hand, such as the disturbance force rejection [2], [4], [10], the manipulability of the grasped object [3], [11], the grasp stability [5], [6], and the grasp robustness against the position error of the contact point [1], [9]. However, few criteria concerning the manipulation task accuracy have been discussed [15]. In this paper, a novel evaluation criterion is introduced to find a grasp configuration with high accuracy in the proposed grasp planning.

This paper is organized as follows. Section II derives basic formulas for a manipulation system. Section III proposes the evaluation criteria for the manipulation task accuracy. Section IV shows the grasp planning method based on dynamics shaping. After several simulations concerning a peg-in-hole insertion task are shown to verify the validity of the grasp planning in Section V, we conclude this paper in Section VI.

## II. Modeling of Manipulation System

### A. Kinematics of Manipulation System

We consider a manipulation system in the three dimensional space, which consists of an object and a multi-fingered hand. It is assumed that the multi-fingered hand has no redundancy, each finger of which has three joints and has contact with the object at the fingertip. The example of such

a robot hand is the NDA Hand as shown in Fig. 1, which was developed in our laboratory [14].

The vector $\boldsymbol{x}_O \in \Re^6$ denotes the position and orientation of the object, whose frame is fixed to the object's center of mass. Let $\boldsymbol{\theta} \in \Re^{3n_f}$ be the vector of the joint angles for the $n_f$-fingers. Assuming that sliding does not occur at any contact points by applying appropriate contact forces, the velocity constraints between $\dot{\boldsymbol{x}}_O$ and $\dot{\boldsymbol{\theta}}$ can be described as

$$\boldsymbol{W}^T \dot{\boldsymbol{x}}_O = \boldsymbol{J}\dot{\boldsymbol{\theta}} \tag{1}$$

Since each finger has three joints as mentioned above, the Jacobian matrix $\boldsymbol{J} \in \Re^{3n_f \times 3n_f}$ becomes a square matrix. The matrix $\boldsymbol{W}^T \in \Re^{3n_f \times 6}$ is the wrench matrix, which relates $\dot{\boldsymbol{x}}_O$ to the velocity of contact points on the object surface.

In a manipulation task by the multi-fingered hand, it is important to control the motion of a task coordinate on the object rather than that of the center of mass of the object, as shown in Fig. 1. The position of the task coordinate, $\boldsymbol{p} \in \Re^3$, can be described using the position and orientation of the object $\boldsymbol{x}_O$ as

$$\boldsymbol{p} = \boldsymbol{p}\left(\boldsymbol{x}_O\right) \tag{2}$$

### *B. Dynamics of Manipulation System*

The equation of motion for the multi-fingered hand can be described as

$$\boldsymbol{M}_H\ddot{\boldsymbol{\theta}} + \boldsymbol{h}_H + \boldsymbol{g}_H = \boldsymbol{\tau} + \boldsymbol{d} - \boldsymbol{J}^T\boldsymbol{f} \tag{3}$$

where $\boldsymbol{M}_H \in \Re^{3n_f \times 3n_f}$ is the inertia matrix, $\boldsymbol{h}_H \in \Re^{3n_f}$, $\boldsymbol{g}_H \in \Re^{3n_f}$, $\boldsymbol{\tau} \in \Re^{3n_f}$, $\boldsymbol{d} \in \Re^{3n_f}$ and $\boldsymbol{f} \in \Re^{3n_f}$ are the vectors of the Coriolis term, the gravitational term, joint torques, unknown disturbance torques and the contact forces exerted by the fingertips, respectively.

The equation of motion for the object can be written as

$$\boldsymbol{M}_O\ddot{\boldsymbol{x}}_O + \boldsymbol{h}_O + \boldsymbol{g}_O = \boldsymbol{W}\boldsymbol{f} \tag{4}$$

where $\boldsymbol{M}_O \in \Re^{6\times 6}$ is the inertia matrix of the object, and $\boldsymbol{h}_O \in \Re^6$ and $\boldsymbol{g}_O \in \Re^6$ are the vectors of the Coriolis and gravitational terms, respectively.

The contact forces, which generate the object's acceleration, can be derived from (4), which are

$$\boldsymbol{f} = \boldsymbol{W}^\sharp(\boldsymbol{M}_O\ddot{\boldsymbol{x}}_O + \boldsymbol{h}_O + \boldsymbol{g}_O) + \boldsymbol{E}\boldsymbol{f}_I \tag{5}$$

where $\boldsymbol{W}^\sharp$ is the pseudo inverse of the wrench matrix $\boldsymbol{W}$, $\boldsymbol{E}$ is a matrix satisfying $\boldsymbol{W}\boldsymbol{E} = \boldsymbol{0}$, and $\boldsymbol{f}_I \in \Re^{3n_f-6}$ represents the magnitude of internal forces.

Since the Jacobian matrix $\boldsymbol{J}$ is invertible unless the robot hand gets into a singular configuration, differentiating (1) yields the joint angular acceleration $\ddot{\boldsymbol{\theta}}$, which is

$$\ddot{\boldsymbol{\theta}} = \boldsymbol{J}^{-1}(\boldsymbol{W}^T\ddot{\boldsymbol{x}}_O + \dot{\boldsymbol{W}}_O^T\dot{\boldsymbol{x}}_O - \dot{\boldsymbol{J}}\dot{\boldsymbol{\theta}}) \tag{6}$$

Substituting (5) and (6) into (3) yields the dynamic equations for the whole manipulation system, which are

$$\boldsymbol{M}_{\text{sys}}\begin{bmatrix} \ddot{\boldsymbol{x}}_O \\ \boldsymbol{f}_I \end{bmatrix} = \boldsymbol{\tau} + \boldsymbol{d} - \boldsymbol{h}_{\text{sys}} - \boldsymbol{g}_{\text{sys}} \tag{7}$$

where $\boldsymbol{M}_{\text{sys}}$, $\boldsymbol{h}_{\text{sys}}$ and $\boldsymbol{g}_{\text{sys}}$ indicate the inertia matrix, and the vectors of the Coriolis term and the gravitational term for the whole manipulation system, respectively.

Since $\boldsymbol{M}_{\text{sys}} \in \Re^{3n_f \times 3n_f}$ is a square matrix, (7) can be solved uniquely for $[\ddot{\boldsymbol{x}}_O^T \ \boldsymbol{f}_I^T]^T$ unless the $\boldsymbol{M}_{\text{sys}}$ becomes singular.

In order to avoid slipping at contact points, it is required that the internal forces should be applied to the object so that the following friction constraint can be satisfied at each contact point $i$.

$$\|\boldsymbol{f}_{ti}\| \le \mu_i f_{ni}, \quad f_{ni} \ge 0 \tag{8}$$

where $f_{ni}$ and $\boldsymbol{f}_{ti}$ are the normal and tangential contact forces, respectively.

Assuming that the manipulation system is a force-closure grasp [7], the robot hand can exert arbitrary internal forces which satisfy the friction constraint (8) on the object.

## III. Manipulation Task Accuracy

### *A. Linearized Dynamic Model*

Uncertainties such as joint friction, mechanical backlash, unpredictable external force etc., which are not shown explicitly in the model of the manipulation system, are imposed on the manipulation system as unknown disturbances, affecting the manipulation accuracy of the task coordinates. In contrast, the exact physical parameter values of the manipulation system are assumed to be known by parameter identification.

A linear system theory is used to analyze the sensitivity of the task coordinate position to unknown disturbances. To begin with, the linearized model of the manipulation system is derived in this section. We regard (2) and (7) with $\boldsymbol{d} = 0$ as the nominal model of the manipulation system. Linearizing the nominal model with respect to equilibrium points yields the state equation and output equation of the manipulation system with the state vector $\Delta\boldsymbol{z} = \left[\ \Delta\boldsymbol{x}_O^T \quad \int\Delta\boldsymbol{f}_I^T dt \quad \Delta\dot{\boldsymbol{x}}_O^T \quad \Delta\boldsymbol{f}_I^T\ \right]^T$ and the output vector $\Delta\boldsymbol{p}$ as follows:

$$\Delta\dot{\boldsymbol{z}} = \boldsymbol{A}\Delta\boldsymbol{z} + \boldsymbol{B}\Delta\boldsymbol{\tau} \tag{9}$$

$$\Delta\boldsymbol{p} = \boldsymbol{C}\Delta\boldsymbol{z} \tag{10}$$

where

$$\boldsymbol{A} = \begin{bmatrix} \boldsymbol{0}_{3n_f\times 3n_f} & \boldsymbol{I}_{3n_f} \\ -\boldsymbol{M}_{\text{sys}}^{-1}\boldsymbol{G} & \boldsymbol{0}_{3n_f\times 3n_f} \end{bmatrix}, \quad \boldsymbol{B} = \begin{bmatrix} \boldsymbol{0}_{3n_f\times 3n_f} \\ \boldsymbol{M}_{\text{sys}}^{-1} \end{bmatrix}$$
$$\boldsymbol{C} = \begin{bmatrix} \boldsymbol{P} & \boldsymbol{0}_{3\times 6(n_f-1)} \end{bmatrix} \tag{11}$$

the matrix $\boldsymbol{I}_i$ is an $i\times i$ identity matrix, $\boldsymbol{0}_{i\times j}$ is an $i\times j$ zero matrix, $\boldsymbol{P} = \partial\boldsymbol{p}/\partial\boldsymbol{x}_O \in \Re^{3\times 6}$, and $\boldsymbol{G} = \partial\boldsymbol{g}_{\text{sys}}/\partial\boldsymbol{x}_O$.

Reference [8] shows the detail derivation of the linearized model of the manipulation system. The motion of the manipulation system is required to be slow so that the linearized model may be valid. In general, the object is manipulated at a slow speed by the multi-fingered hand in the case of a precise manipulation as discussed in this paper.

### B. Evaluation for Manipulation Task Accuracy

A system $(\boldsymbol{A}, \boldsymbol{B}, \boldsymbol{C})$ is said to be output controllable if it is possible to construct control inputs that will transfer any given initial output to any final output within a finite time interval. An output controllability matrix of the system with $2n$-state variables can be expressed by

$$\boldsymbol{N} = \boldsymbol{C}[\boldsymbol{B}\ \boldsymbol{A}\boldsymbol{B}\ \cdots \boldsymbol{A}^{2n-1}\boldsymbol{B}]. \tag{12}$$

The output controllability is evaluated by using the singular value and the singular vector of the output controllability matrix.

Substituting (11) into (12) yields the output controllability matrix of the manipulation system, which relates the set of output controllable task coordinate position to the set of applied joint torque within a finite time interval.

The sensitivities of the task coordinate position to joint torques are maximal and minimal in the directions of the singular vectors corresponding to the maximum and minimum singular values of the output controllability matrix, respectively, the directions of which are perpendicular to each other.

Therefore, if the joint torques contain unknown disturbances, the sensitivity of the task coordinate position to the unknown disturbances is maximal in the direction of the maximum singular vector. In contrast, its sensitivity is minimal in the direction of the minimum singular vector.

Hence, since the task coordinate positions are to be distributed along near the maximum singular vector due to the unknown disturbances, the manipulation task accuracy along its direction becomes the worst. On the contrary, since the distribution of the task coordinate position along the minimum singular vector is most suppressed, the manipulation task accuracy along the direction becomes the best.

Meanwhile, the degrees of distribution of the task coordinate position are given by the condition number of the output controllability matrix as

$$c = \sigma_{\max}/\sigma_{\min}\ \geq 1.0 \tag{13}$$

The larger the condition number is, the higher the sensitivity to the unknown disturbance along the maximum singular vector becomes. Therefore, the task coordinate position converges more along the direction of the maximum singular vector. In contrast, since the sensitivity to the unknown disturbance along the minimum singular vector becomes lower, the distribution along the minimum singular vector is much suppressed. Thus, the manipulation task accuracy is improved along the direction of the minimum singular vector.

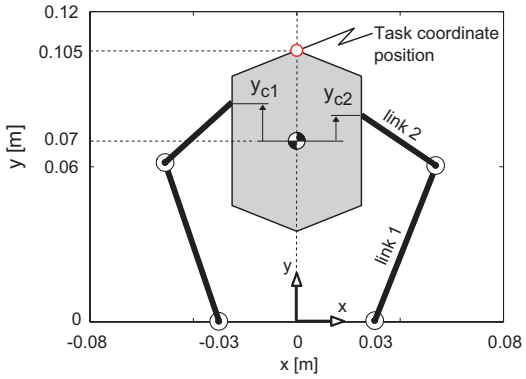


Fig. 2. The two-fingered hand grasping a hexagonal object

TABLE I
PHYSICAL PARAMETERS

| | |
|---|---|
| Object's mass | 66.0 g |
| Link 1 and Link 2 | 6.5 cm, 3.5 cm |
| Link's line density | 10 g/cm |
| Friction coefficient: $\mu$ | 0.5 |
| Internal force: $f_I$ | 10 N |

From the mentioned above, the task manipulation accuracy is evaluated by the direction of the singular vectors and the condition number. It is considered that the internal force, which is a contact force that does not contribute to the object motion, has no influence on the task manipulation accuracy, since it is assumed in this paper that there is no limitation for the range of joint driving torques and that the robot hand can generate the internal force against any disturbance so that the friction constraint (8) can be satisfied. Next, we show some simulation examples.

### C. Simulation Examples

Fig. 2 shows a two-fingered hand which grasps a hexagonal object in a horizontal plane. The robot hand consists of the same two fingers, each of which has two joints. Therefore there is no redundancy in this manipulation system. It is assumed that the position and orientation of the object are fixed, while the left and right contact points locating at $y_{c1}$ and $y_{c2}$ from the center of mass of the object are changed. The task coordinate position is set at the top vertex of the object. Table I shows the physical parameters of the manipulation system.

In the initial grasp configuration, the robot hand grasps the object stably with the appropriate internal forces which satisfy the friction constraint. The displacement of the task coordinate position caused by disturbance torques applied to the joints during an infinitesimal time is calculated by using (2) and (7). We obtain the distribution of the task coordinate position by repeating this process 50 times and analyze the

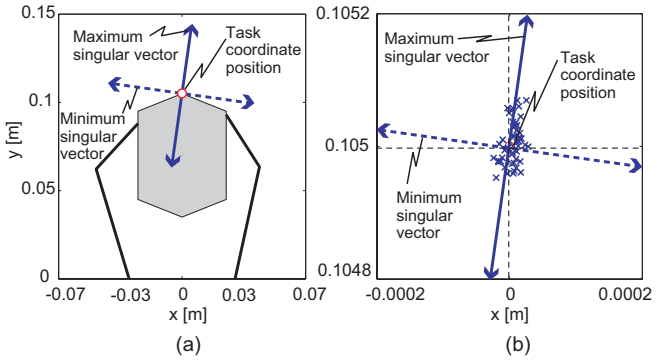


Fig. 3. (a) Grasp configuration with $y_{c1}$=1.8 cm and $y_{c2}$=2.3 cm. (b) Distribution of task coordinate position. $c = 2.0$.

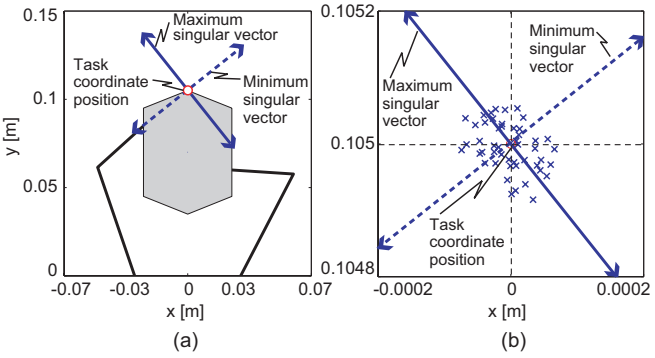


Fig. 4. (a) Grasp configuration with $y_{c1} = 1.5$ cm and $y_{c2} = -1.0$ cm. (b) Distribution of task coordinate position. $c = 1.3$.

direction and convergence of the distribution to evaluate the manipulation task accuracy.

It is assumed that the disturbance torques are white noise, the average and variance of which are zero and $0.02\text{N}^2\text{m}^2$, respectively, and the execution time is $t_f = 10$ msec. The internal forces and contact points are set so as to satisfy two-finger force-closure grasp condition [7].

First, we discuss the case of Fig. 3(a), where the initial grasp configuration is $y_{c1}$=1.8 cm and $y_{c2}$=2.3 cm. The arrows attached at the task coordinate position indicate the directions of the maximum and minimum singular vectors, respectively. By applying the disturbance torques to this manipulation system repeatedly, the distribution of the task coordinate position is obtained, which is denoted by $\times$ in Fig.3(b). The center of this figure indicates the initial task coordinate position. The heavy and dash lines indicate the maximum and minimum singular vectors, respectively. As seen from the simulation result, the task coordinate position converges along near the maximum singular vector, while the distribution along the minimum singular vector is suppressed.

When the initial grasp configuration is changed by shifting the contact position from Fig. 3(a) to Fig. 4(a), the directions of the singular vectors change significantly and the condition number decreases from 2.0 to 1.3. As seen from Fig. 4(b), although the task coordinate position distributes along near the maximum singular vector, its convergence becomes lower than that of Fig. 3(b). This means that the task coordinate position spreads more along the minimum singular vector, because the condition number becomes smaller.

These simulations reveal that the manipulation task accuracy depends on the direction of the singular vectors and the condition number of the output controllability matrix for the manipulation system.

## IV. Grasp Planning based on Dynamics Shaping

The output controllability matrix of the manipulation system consists of the wrench matrix, the Jacobian matrix and the hand inertia matrix, as seen from (11) and (12). It is found that the manipulation task accuracy depends on the grasp configuration such as the contact position, the hand configuration and the object's position and orientation. We propose a novel grasp planning which finds the grasp configuration with high manipulation task accuracy, which is called "dynamics shaping" [12].

As a simulation example, Fig. 5 shows the maximum singular vectors for the $20 \times 20$ grasp configurations, which are obtained by changing the contact positions $y_{c1}$ and $y_{c2}$ by $0.15$ cm step size within the range of $\pm 1.5$ cm. This simulation indicates that the direction of the singular vector as well as the condition number can be set arbitrarily by dynamics shaping under the condition that the dynamics and kinematics of the manipulation system are satisfied.

In the case of a tool manipulation or a peg-in-hole task, the directions in which the high positional precision is required are designated in advance. If the grasp configuration can be planned to suppress the positional error in the directions where the high positional precision is required, it is possible to avoid the collision between the object and an environment as much as possible and achieve a robust manipulation task against unknown disturbances.

In order to obtain such a robust grasp configuration, a grasp planning procedure based on dynamics shaping is described as follows:

1) To find grasp configurations such that the minimum singular vector points toward the direction where high positional precision is required.

2) To select a grasp configuration the condition number of which is the largest among those satisfying the condition 1).

The next section shows application examples of the proposed grasp planning.

## V. Grasp Planning for Peg-in-hole Task

The peg-in-hole task is often seen in a parts assembly. Here, we find an optimal grasp configuration for a two-fingered hand to insert an object, as shown in Fig. 6. The task frame is fixed at the top vertex of the cone of the inserted

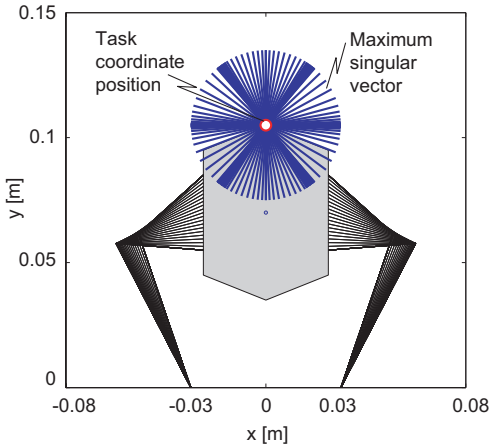


Fig. 5. Change of direction of maximum singular vectors according to the change of grasp configuration

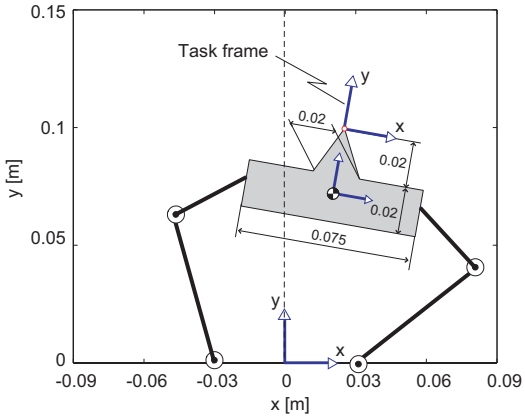


Fig. 6. Peg-in-hole task by two-fingered hand

object, the $x$ axis of which points toward the direction where high positional precision is required. The direction of the $y$ axis is set based on the right-handed coordinate system. Let the origin of the hand frame, which is regarded as the base frame in this simulation, be attached at the middle point between two base joints and the origin of the object frame be attached at the center of mass of the object.

The grasp configuration shown in Fig. 6 is determined by the object's position and orientation with respect to the hand frame and the contact position on the object's surface. Thus the grasp planning in this simulation is defined as the problem to find the object's position and orientation and the contact position which minimize the error generation as much as possible along the direction where the positional precision is required (the direction of $x$-axis in the task frame). Therefore, the optimal grasp configuration with respect to the hand frame is obtained in this simulation. Assuming that the robot hand is installed at the end of a robot arm, the robot hand should be moved by the robot arm so that $y$-axis of task frame points toward the direction of insertion.

Let the search range of the object's position and orientation $(x,\ y,\ \phi)$ with respect to the hand frame be respectively $-0.05 \leq x \leq 0.05$ m, $0.05 \leq y \leq 0.1$ m and $-\pi/2 \leq \phi \leq \pi/2$ rad and these step sizes be 1.0 cm, 1.0 cm and 0.035 rad, respectively. The search range of the contact points is on the entire surfaces of the object except the cone. Its step size is 0.5 mm. To keep the contact points away from the vertices of the object, the 5 mm edge from both ends of all edges is eliminated from the search range. Other conditions for the simulation are same as Section III-C.

[Example 1] Fig. 7(a) shows the optimal grasp configuration for the peg-in-hole insertion task derived from the planning. The object's mass is 45.1 g and other physical parameters are shown in Table I.

In this grasp configuration, the minimum singular vector points toward the $x$-axis of the task frame, the direction of which requires the positional precision. Since the object's shape is axisymmetric about the $y$-axis of the task frame, the optimal grasp configuration becomes symmetric. The distribution of the task coordinate position caused by the unknown disturbance is denoted by $\times$ in Fig. 7(b). The arrows indicate the task frame of the initial grasp configuration. As seen from this figure, the distribution along the $x$-axis of the task frame is suppressed. This means that the obtained grasp configuration is suitable for the peg-in-hole insertion.

Next, we consider a optimal grasp configuration for the object shown in Fig. 8, the cone of which is just moved from the center to the right of the object. The object has same mass as the object in Fig. 7. The task frame is attached at the top of the cone.

Since the object is asymmetry unlike the object in Fig. 7, the optimal grasp configuration is also asymmetry as shown in Fig. 8(a). The distribution along the $x$-axis of the task frame is suppressed as shown in Fig. 8(b). This means that the appropriate grasp configuration is obtained.

[Example 2] Consider a optimal grasp configuration for the L-shaped object shown in Figs. 9 and 10. Only the direction of the task frame where the positional precision is required is different. The object's mass is 32.4 g and other physical parameters are same as shown in Table I.

Figs. 9(a) and 10(a) show the optimal grasp configuration obtained by the planning. The minimum singular vectors of them point toward the $x$-axis of each task frame. Figs. 9(b) and 10(b) show that the distribution along $x$-axis of each task frame is suppressed. As seen from these simulation results, even if the direction of the task frame is changed, the proposed grasp planning method can find the optimal grasp configuration so that the error along the newly specified direction which requires the positional precision can be suppressed.

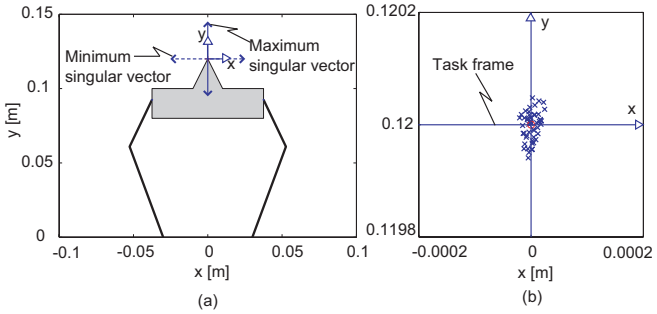


Fig. 7. Example 1. (a) Optimal grasp configuration. (b) Distribution of task coordinate position. $c = 2.8$.

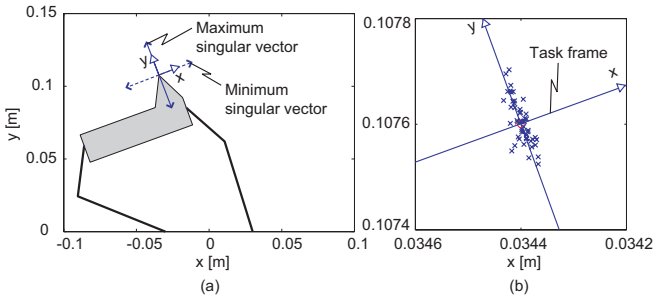


Fig. 8. Example 1. (a) Optimal grasp configuration. (b) Distribution of task coordinate position. $c = 3.7$.

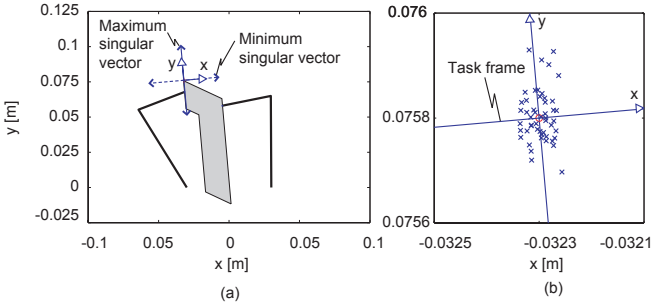


Fig. 9. Example 2. (a) Optimal grasp configuration. (b) Distribution of task coordinate position. $c = 2.5$.

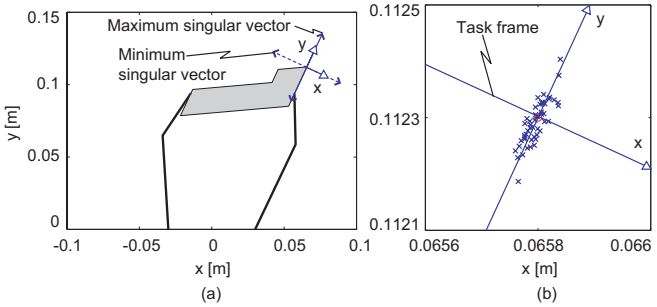


Fig. 10. Example 2. (a) Optimal grasp configuration. (b) Distribution of task coordinate position. $c = 3.8$.

## VI. Conclusion

This paper revealed the following:

(1) The manipulation task accuracy of a robot hand system against unknown disturbances is determined by the direction of the singular vector and condition number of the output controllability matrix for the manipulation system.

(2) The grasp planning based on dynamics shaping has been proposed, which finds a grasp configuration so that the error of the task coordinate position toward the direction where the high positional precision is required can be suppressed.

(3) The validity of the grasp planning has been shown by several simulations concerning a peg-in-hole insertion task.

Our future works are as follows: analysis for the orientation error of the task coordinate, consideration to collision between the object and environment, and experiments using the NDA hand.

## References


[1] G.M. Bone and Y. Du, "Multi-Metric Comparison of Optimal 2D Grasp Planning Algorithms," *Proc. of the IEEE International Conference on Robotics and Automation*, pp.3061-3066, 2001.

[2] C. Borst, M. Fischer and G. Hirzinger, "Grasp Planning: How to Choose a Suitable Task Wrench Space," *Proc. of the IEEE International Conference on Robotics and Automation*, pp.319-325, 2004.

[3] P. Chiacchio, S. Chiaverini and B. Siciliano, "Global Task Space Manipulability Ellipsoids for Multiple-Arm Systems," *IEEE Journal of Robotics and Automation*, Vol.7, No.5, pp.678-685, 1991.

[4] C. Ferrari and J. Canny, "Planning Optimal Grasps," *Proc. of the IEEE International Conference on Robotics and Automation*, pp.2290-2295, 1992.

[5] W.S. Howard and V. Kumar, "On the Stability of Grasped Objects," *IEEE Transaction of Robotics and Automation*, Vol.12, No.6, pp.904-917, 1996.

[6] Q. Lin, J.W. Burdick and E. Rimon, "A Stiffness-based quality Measure for Compliant Grasps and Fixtures," *IEEE Transaction of Robotics and Automation*, Vol.16, No.6, pp.675-688, 2000.

[7] V-D. Nguyen, "Constructing Force-Closure Grasps," *The International Journal of Robotics Research*, Vol.7, No.3, pp.3-16, 1988.

[8] D. Prattichizzo and A. Bicchi, "Dynamic Analysis of Mobility and Graspability of General Manipulation Systems," *IEEE Transaction of Robotics and Automation*, Vol.14, No.2, pp.241-258, 1998.

[9] M.A. Roa and R. Suarez, "Computation of Independent Contact Regions for Grasping 3-D Objects," *IEEE Transaction of Robotics*, Vol.25, No.4, pp.839-850, 2009.

[10] M. Strandberg and B. Wahlberg, "A Method for Grasp Evaluation Based on Disturbance Force Rejection," *IEEE Transaction of Robotics*, Vol.22, No.3, pp.461-469, 2006.

[11] T. Watanabe, "Joint Torque-velocity Pair Based Manipulability for Grasping System," *Proc. of the IEEE/RSJ International Conference on Intelligent Robots and Systems*, pp.2264-2270, 2008.

[12] T. Yamawaki, Y. Tsuzuki and M. Yashima, "Robust Hitting with Dynamic Shaping," *Proc. of the IEEE International Conference on Robotics and Automation*, pp.114-119, 2009.

[13] T. Yamawaki and M. Yashima, "Planning Tracking Motion Insusceptible to Unknown Disturbances Using Sensitivity Measure," *Proc. of the IEEE International Conference on Robotics and Biomimetics*, pp.1571-1576, 2010.

[14] T. Yamawaki, S. Asano, H. Miyashita, and M. Yashima, "Robotic Catching with Precision Grasp by Vision," *Proc. of IEEE International Conference on Robotics and Biomimetics*, pp.909-914, 2008.

[15] M. Yashima and T. Yamawaki, "Task-Oriented Accuracy Measure for Dexterous Manipulation," *Proc. of IEEE International Conference on Robotics and Biomimetics*, pp. 903-908, 2008.